Final Draft
of the original manuscript:

Zbytovska, J.; Kiselev, M.A.; Funari, S.S.; Haramus, V.M.; Wartewig, S.; Palat, K.; Neubert, R.:

Influence of cholesterol on the structure of stratum corneum lipid model membrane

In: Colloids and Surfaces A (2008) Elsevier

DOI: 10.1016/j.colsurfa.2008.06.032

Influence of cholesterol on the structure of stratum corneum lipid model membrane

J. Zbytovská[1, 2*], M.A. Kiselev[2, 3], S. S. Funari[4], V. M. Garamus[5], S. Wartewig[6], K. Palát[7], R. Neubert[2]

1 Department of Pharmaceutical Technology, Faculty of Pharmacy, Charles University in Prague, Heyrovského 1203, 50005 Hradec Králové, Czech Republic

2 Department of Pharmacy, Martin-Luther-University Halle-Wittenberg, Wolfgang-Langenbeck Str. 4, D-06120 Halle/Saale, Germany

3 Frank Laboratory of Neutron Physics, Joint Institute for Nuclear Research, Dubna 141980, Russia

*4 Max Planck Institute of Colloids and Interfaces, Am Muehlenberg 1, 14476 Golm, *c/o HASYLAB, Hamburg, Germany*

5 GKSS Research Centre, Max-Planck-Str., D-21502, Geesthacht, Germany

6 Institute of Applied Dermatopharmacy, Wolfgang-Langenbeck Str. 4, D-06120 Halle/Saale, Germany

7 Department of Inorganic and Organic Chemistry, Faculty of Pharmacy, Charles University in Prague, Heyrovského 1203, 50005 Hradec Králové, Czech Republic

*Corresponding author: Faculty of Pharmacy, Charles University in Prague
Department of Pharmaceutical Technology
Heyrovského 1203
50005 Hradec Králové
Czech Republic
Tel. No.: +420 495067383
Fax No.: +420 495518002
E-mail address: zbytovska@faf.cuni.cz

Abstract

This study describes the influence of cholesterol on a model membrane consisting of four stratum corneum (SC) lipids: ceramide [AP], cholesterol, palmitic acid and cholesterol sulphate. Using small-angle X-ray diffraction (SAXD) on multilamellar vesicles (MLVs), the lamellar repeat distance, D, was determined. Small-angle neutron scattering (SANS) on unilamellar vesicles (ULVs) was used to obtain the membrane thickness and the average area of the membrane surface per molecule. Immediately after the sample preparation, the membranes show one lamellar phase. During next days, the systems separate into two lamellar phases and crystalline cholesterol. On heating the samples to 85 °C, the domains merge into one phase, the D-value of which increases slightly with increasing cholesterol concentration. On cooling the samples to 32 °C, only one phase is observable again. Unlike at high temperatures, D decreases with increasing cholesterol content. The membrane thickness determined by SANS decreases and the area of the membrane surface per molecule increases with increasing cholesterol concentration in the membranes. Likely, cholesterol fluidises the SC lipid membranes in the mixed state at 32 °C after heating and condenses the membranes at 85 °C.

Keywords: stratum corneum lipids, cholesterol, X-ray diffraction, neutron scattering, multilamellar and unilamellar vesicles

1 Introduction

The skin barrier plays an essential role in the protection of body against xenobiotics from the environment and against water evaporation from the organism. Stratum corneum (SC), the outermost skin layer, is responsible for the permeability properties of mammalian skin. This membrane consists of keratin-rich corneocytes embedded in a lipid matrix with a lamellar organization. Ceramides of nine types, free fatty acids, cholesterol and its derivatives are the most abundant lipids in the SC [1].

The SC lipids show a complex behaviour, which is dependent on the particular lipid composition in the SC matrix. In diseased skin, a deviation in lipid composition has often been found. The recessive X-linked ichthyosis (RXLI) is associated with the steroid sulphatase deficiency; the enzyme which converts sulphated steroids to steroids [2]. Due to this, increased levels of cholesterol sulphate (CS) connected with decreased levels of cholesterol (CHOL) were found in the affected skin [3]. Although the CS accumulation seems to be the primary mechanism contributing to the barrier abnormalities in RXLI, the reduced CHOL levels play also an important role especially in the altered membrane dynamics. Topically administrated CHOL reverses the pathologic effects of excess CS on SC membrane structure, barrier function, and desquamation [4]. Additionally, ichthyotic symptoms were induced by cholesterol-lowering drugs [5].

Although there are several studies focusing on the role of CHOL in the SC [6,7,8,9], the influence of CHOL on the SC lipid membrane structure still requires a complete elucidation.

The present study describes the effect of CHOL on a model membrane imitating the native SC lipid matrix. This model consists of ceramide [AP] (Cer[AP]), palmitic acid, CHOL and CS. Besides the usual small-angle X-ray diffraction (SAXD) on multilamellar vesicles (MLVs), the small-angle neutron scattering (SANS) is applied. SANS is not an unusual method in the studies on various phospholipid systems [10,11]; it has been, however, rarely employed in the skin characterisation. The very small-angle neutron scattering (VSANS) has been successfully applied to study the water sorption [12] and to mathematically determine some

structural features of SC [13]. Similarly, the neutron diffraction on native SC [14,15] and multilamellar SC lipid films [16] allows to study the SC membrane structure and hydration. Nevertheless, SANS has been reported not to be the ideal method when used on the native SC due to the high complexity of the system [17].

In this context, SANS on a more simple system such as unilamellar vesicles (ULVs) of a SC lipid model membrane is employed in this study. Using the 'model of separated form factors' developed for phospholipid vesicles [18] and the the Kratky-Porod analysis of the Guinier approximation [19,20], the membrane thickness parameter, d, and the average area per molecule of the membrane surface have been determined. The influence of cholesterol on these membrane parameters and on the lamellar repeat distance, D, gained from the SAXD measurements is described.

2 Material and Methods

2.1 Material

N-α-Hydroxyoctadecanoylphytosphingosine (Cer [AP]; see Fig. 1) was a gift from Cosmoferm (Delft, The Netherlands). Cholesterol (CHOL), cholesterol sulphate (CS), and palmitic acid, as well as Trizma® (Tris) buffer, and sodium chloride were purchased from Sigma-Aldrich (Taufkirchen, Germany). D_2O (99.98% deuteration) was purchased from Chemotrade (Leipzig, Germany). Water, chloroform and methanol used were of HPLC grade.

2.2 Vesicle Preparation

The composition of the lipid system used in this study was chosen regarding previous data [21,22]. A basic system that should mostly imitate the real SC lipid composition consists of 55% (in weight) Cer[AP], 25% CHOL, 15% palmitic acid and 5% CS (mixture IV). The other samples were prepared varying the proportion of CHOL (from 10 to 30%), the relative ratio of other lipids remaining constant. The samples used in the study are listed in Table 1.

MLVs were prepared by the 'thin layer method' [23]. The lipids were dissolved separately in chloroform/methanol mixture 2/1 (in volume). The required amounts of the solutions were mixed together and dried down using a rotary evaporator. To remove the rest of the solvent, the samples were kept under vacuum for one day. An appropriate amount of 10 mM Tris buffer, pH = 9.0 with 100 mM NaCl in water or in D_2O was added to the dry sample. The samples were then heated for one hour to 90 °C and mixed on a vortex every 20 min till a milky MLV suspension was formed.

The ULVs were prepared from the MLV suspension by extrusion through polycarbonate filters with a pore diameter of 500 Å at 75 °C using a LiposoFast Basic extruder from Avestin (Ottawa, Canada).

2.3 Vesicle characterization

The concentration of lipids in the ULVs after extrusion was determined by high performance thin layer chromatography (HPTLC) using Automatic TLC Sampler 4, AMD 2 development chamber and TLC scanner 3 (Camag, Muttenz, Switzerland) according to Farwanah [24] . Integration and quantification based on peaks areas were performed using CATS software (Camag).

The size and stability of prepared ULVs (1% w/w of lipids in buffer) was checked by photon correlation spectroscopy using a particle size analyser (Malvern HPPS-ET, Malvern Instruments, UK). The measurements were carried out at 32 °C. The hydrodynamic radius and the polydispersity have been calculated from the correlation function by the CONTIN algorithm using the HPPS-Malvern program for dispersion technology and light scattering systems.

2.4 Small Angle X-ray Diffraction

Small angle X-ray diffraction (SAXD) data were collected on the Soft Condensed Matter beamline A2 of HASYLAB at the storage ring Doris III of the Deutsches Elektronen

Synchrotron. A two-dimensional CCD detector was used for data acquisition. The MLVs with 20% (w/w) lipid concentration in Tris buffer with 100 mM sodium chloride were measured ten days after preparation at 32, 85, and 32 °C again in specially designed copper cells with a polyimid-foil (Kapton®, DuPont, Luxembourg) window (50 µl in volume). The sample-to-detector distance was 585 mm and the X-ray wavelength was 1.5 Å. The acquisition time of each sample was 3 minutes. Silver behenate and rat tendon tail collagen were used for calibration. Prior to each measurement, the sample was allowed to equilibrate for 10 minutes.

The data evaluation was carried out using the FIT2D software. The scattering intensity was measured as a function of scattering vector, q. The latter is defined as $q = (4\pi/\lambda)\sin\Theta$, where 2θ is the scattering angle and λ is the X-ray wavelength. The lamellar repeat distance, D, was calculated from the first order diffraction peak according to $D = 2\pi/q$. Using a Lorentzian function, the diffraction peaks were fitted to determine the exact positions. This function was chosen instead of the usual Gaussian one because of the higher fit accuracy.

A STOE STADI-IV diffractometer (Stoe and Cie, Darmstadt, Germany) equipped with CuK_α radiation (wavelength 1.54 Å) and a linear position sensitive detector was used to measure the samples about 3 hours after the preparation. The samples were placed in a quartz capillary and measured in a transmission geometry at 20 °C with the 2Theta angle moving between 0 to 6 degrees for two hours.

2.5 Small Angle Neutron Scattering

The ULVs with 1% (w/w) lipid concentration in Tris buffer in D_2O adjusted to pH 9 were measured at the neutron wavelength of 8.1 Å at the SANS 1 spectrometer of the Geesthacht Neutron Facility, GKSS Research Centre, Germany. To receive scattering curves in a broad q range, four sample-to-detector distances of 70.5, 180.5, 450.5, and 970.5 cm were used. The data were collected at 32 °C. The acquisition time at 70.5 cm was 1 hour, at other

sample-to-detector distances 0.5 hour. For background subtraction, the scattering curve of the relevant buffer has been used, which was measured on the same way as the sample.

The analysis of the SANS curves has been achieved using two methods, namely the 'model of separated form factors' [18], and the Kratky-Porod analysis of the Guinier approximation [19,20,25].

According to the "model of separated form factors", the macroscopic cross section of the monodispersed population of ULVs is given by:

$$\frac{d\Sigma(q)}{d\Omega_{mon}} = nF_s(q,R)F_b(q,d)S(q) \qquad (1)$$

where n is the number of vesicles per unit volume, $F_s(q,R)$ is the form factor of the infinitely thin sphere with the radius R

$$F_s(q,R) = \left(4\pi\frac{R^2}{qR}\sin(qR)\right)^2 \qquad (2)$$

$F_b(q,d)$ is the form factor of the symmetrical lipid bilayer with the thickness d, which can be expressed by

$$F_b(q,d) = \left(\frac{2\Delta\rho}{q}\sin\left(\frac{qd}{2}\right)\right)^2 \qquad (3)$$

for the case of a bilayer with constant scattering length density across the membrane ρ(x)=const. $\Delta\rho$ is the neutron contrast. $S(q)$ is structure factor of the vesicle population. For the used lipid concentrations 1% (w/w) this factor is $S(q) \approx 1$ [26].

The average vesicle radius R can be calculated from the scattering curve based on Eq. (2) as $R = \pi/q_{R\min}$, where q_{Rmin} is the first minimum in the form factor of infinitely thin sphere after averaging of the population of polydisperse vesicles.

The membrane thickness parameter *d* can be directly calculated from the position q_0 of the first minimum of the sine function in the Eq. (3) as $q = 2\pi / q_{d\min}$. For a membrane thickness of about 30 Å, the position of q_{dmin} is about 0.2 $Å^{-1}$ [27].

Another possibility to calculate the membrane thickness from a scattering curve offers the Guinier approximation [19,20,25]. In the *q* range valid for a homogeneous membrane approximation, the scattering intensity of ULVs dispersed in heavy water can be given by:

$$I(q) = 2\pi I(0) q^{-2} \exp\left(-q^2 R_t^2\right) \qquad (4)$$

where *I(0)* is scattering to "zero angle" and R_t is membrane gyration radius. In this approach, the R_t parameter is the absolute value of the slope of the Kratky-Porod plot ($ln[I(q)q^2]$ vs q^2) and the membrane thickness parameter, d_g, can be calculated as

$$d_g^2 = 12 R_t^2 \qquad (5)$$

I(0) cannot be measured experimentally but it can be determined by extrapolation to the zero value of the Kratky-Porod plot. The value of *I(0)* is given by the total particle scattering length, namely, by the sum of the scattering lengths of all atoms inside the particle. Therefore, the chemical composition being known, the evaluation of *I(0)* allows the molecular mass per unit of vesicle surface to be determined [20,28]. In the limit of $q \to 0$, the mass of the membrane per unit of surface, M_s, can be determined by dividing the scattered intensity *I(0)* by the total lipid concentration c and the average scattering length density per unit mass, $\Delta\rho_m$ according to:

$$I(0) = M_s c \Delta\rho_m^2 \qquad (6)$$

The membrane area per molecule, *A*, in centrosymmetric bilayers can be calculated by:

$$A = 2 / \left(M_s N_A / M_W\right) \qquad (7)$$

where M_W is the average molecular weight of the lipids, M_S the determined membrane mass per unit of surface and N_A the Avogadro number.

2.6 Molecular modelling

In order to determine the average excess scattering-length density per unit mass, the molecular volumes were calculated. Quantum-chemical calculations were run on a PC computer using software HyperChem for Windows v. 7.1, Hypercube Inc. The models of compounds were formed on RHF/AM1 level. We used the conformation of Cer[AP] with parallel aliphatic chains calculated as described previously [29]. Solvent accessible volumes, V_{SA}, of models of studied compounds were calculated using the grid method [30] using the atomic radii of Gavezzotti [31]. The solvent probe radius 0.4 Å and 20 points on the cube side were used.

3 Results

3.1 Small Angle X-ray Diffraction from MLVs

Fig. 2 shows the diffraction patterns of the SC lipid model MLVs with 10 and 25% CHOL (mixtures I and IV, respectively) measured immediately after the extrusion. The samples show only one diffraction peak at 0.137 Å for 25% CHOL and 0.131 Å for 10% CHOL, which indicates one phase with the lamellar repeat distance of 45.9 Å and 48.0 Å, respectively.

The diffraction patterns of the SC lipid model systems measured on the synchrotron ten days after the sample preparation with various CHOL concentrations are given in Fig. 3a, b, and c. The obtained results are summarized in Table 2.

At 32 °C before heating, the diffractograms are quite complex (Fig. 3a). The positions of the diffraction peaks indicate that the systems are separated into two lamellar phases, namely a ‘short’ one (the S-phase) with the lamellar repeat distance of about 42 Å and a ‘long’ one (the L-phase) with the lamellar repeat distance of about 47 Å. Both phases induce three diffraction orders in the diffractograms. It is apparent in Fig. 4 that with increasing CHOL content from 10 to 30% the calculated periodicity of the L-phase increases slightly from 46.7±0.2 Å to 47.5±0.2 Å, whereas the periodicity of the S-phase remains almost unchanged.

In all the samples, a small peak is detectable at 0.187 $Å^{-1}$. This peak position corresponds to a repeat distance of 33.6±0.1 Å and was assigned to crystalline CHOL monohydrate [32]. The peak intensity increases with the increasing concentration of CHOL in the mixture, while the position is stable. In the diffractograms of the samples with 25 and 30% CHOL even more diffraction orders of crystalline CHOL monohydrate are detectable.

When the systems are heated to 85 °C (Fig. 3b), the S- and L-phases merge into one phase, whose repeat distance increases with the CHOL content from 41.8±0.2 Å for the sample with 10% CHOL to 42.8±0.2 Å for the sample with 30% CHOL (Fig. 4). Regarding the peak at 0.187 $Å^{-1}$, a small amount of crystalline CHOL is still present particularly in the samples with higher CHOL concentrations.

When the samples are cooled back to 32 °C, they show only one lamellar phase. This phase is strongly affected by the concentration of CHOL in the system. The periodicity decreases almost linearly with increasing CHOL concentration from 47.6±0.2 Å for 10% CHOL to 44.9±0.2 Å for 30% CHOL (Fig. 4). The peak belonging to crystalline CHOL is slightly observable especially in the samples with higher CHOL content.

The recovery of the system with 25% CHOL (mixture IV) into the initial state has been studied further. Fig. 5 shows the X-ray diffraction patterns of the sample measured 20 minutes, 1 day, and 10 days after the heating. 20 minutes after the heating, there is one diffraction peak at 0.138 $Å^{-1}$, which indicates one phase with 45.5 Å. One day later, the sample still shows only one peak at 0.136 $Å^{-1}$ which corresponds to the D-value of 46.2 Å. The diffractogram measured 10 days after the heating shows two peaks indicating the phase separation into the S- and L- phase with 41.9 and 47.3 Å, respectively.

3.2 Characterization of ULVs

The HPTLC analysis of the lipids in the ULV and MLV samples confirms that the substances are stable during the sample preparation and shows that the CHOL content was slightly reduced after the extrusion. The concentration of CHOL in the ULVs is given in brackets in

Table 1. The difference in the proportions of the other lipids in MLVs and ULVs was negligible.

According to DLS studies, all the ULV samples showed a monomodal population with a hydrodynamic radius between 550 - 650 Å and a polydispersity of about 30%. Fig. 6 shows the size distribution of the sample with 25% CHOL (mixture IV). No influence of CHOL concentration in the system on the hydrodynamic radius and the polydispersity was found. The ULVs were stable for at least 7 days at pH 9 and laboratory temperature.

3.3 Molecular modelling and the average scattering length density calculation

The solvent accessible volumes (V_{SA}) were calculated for Cer[AP], CS, CHOL and palmitic acid. The V_{SA}-values amount to 990.59 and 666.86 $Å^3$ for Cer[AP] and CS, respectively. The volumes of CHOL and palmitic acid are 617.12 and 450.27 $Å^3$, respectively, which is comparable with literature data obtained from volumetric measurements [33,34].

The average excess scattering-length density per unit mass ($\Delta\rho_m$) of the lipid mixtures in D_2O was determined from the known chemical composition [35]. The calculated values are listed in Table 3.

3.4 Small Angle Neutron Scattering from ULVs

Fig. 7a shows the neutron scattering curves of the ULVs with various CHOL concentrations. No diffraction peak of a multi- or oligolamellar arrangement or of crystalline CHOL as in the case of MLVs is present.

The minimum of the membrane thickness, q_{dmin}, is distinct at about 0.18 $Å^{-1}$ and shifts its position to higher q-values with the increasing CHOL content. The membrane thickness parameters, d, calculated from the minimum q_{dmin} according to the model of separated form factors with an accuracy of 5% amount to 36.9 Å, 36.4 Å, 35.3 Å, and 34.6 Å for mixture I (9% CHOL), II (14% CHOL), IV (20% CHOL), and V (27% CHOL), respectively (Fig. 8a).

The Kratky-Porod plots of the measured scattering curves (Fig. 7b) show a linear range in the q-range between 0.06 and 0.14 $Å^{-1}$. The slopes of the plots, which correspond to the square of the radius of gyration, decrease with increasing concentration of CHOL in the samples. The membrane thickness parameters, d_g, calculated from the R_g values show the same tendency and amount to 38.7±0.8, 38.2±0.8, 35.3±0.7, and 33.9±0.7 Å for mixture I (9% CHOL), II (14% CHOL), IV (20% CHOL), and V (27% CHOL), respectively (Fig. 8a).

The average area per molecule of the membrane surface has been calculated from the I(0) values. The determined values are 55.2, 57.3, 61.7, and 68.1 $Å^2$ for the samples with 10, 15, 25, and 30% CHOL, respectively. Because the molar volumes were determined by the molecular modelling and not by real measurements, a statistical error can affect the results partway; however, the tendency that the increasing CHOL concentration increases the area per molecule of the membrane surface is obvious (Fig. 8b).

The minimum, q_{Rmin}, related to the average vesicle radius, is not visible in the scattering curves in any of the samples measured.

The data obtained from the SANS measurements are summarized in Table 4.

4 Discussion

This study introduces SANS on ULVs into the methods for the characterization of the SC lipid membranes. In order to carry out those measurements successfully, it was important to prepare stable unilamellar vesicles of a SC lipid model system. The composition was chosen according to previous studies. To create stable ULVs, high pH values of the environment are mandatory [21,36]. At pH = 9, the charged components (palmitic acid and CS in the present system) are fully ionized. Due to this, vesicles can be extruded without a considerable loss of lipids. Contrary to ULVs prepared at pH = 6, vesicles prepared at pH = 9 have been found to be stable for 4-6 weeks [21]. A decrease in the pH to 6 activated vesicle fusion and lysis [37]. Since the SANS measurements take quite a long time (several days), stable ULVs are needed. For this reason, samples with high pH values of the environment were used in our experiments. Consequently, it was possible to apply SANS and to employ the ‘model of

separated form factors' and the Guinier approximation which gave us information about the membrane thickness and membrane density.

The SAXD measurements demonstrate that the SC lipid model system shows complex phase behaviour. Immediately after the preparation, the MLVs show one phase with the lamellar repeat distance of 45.9 Å and 48.0 Å for 25 and 10% CHOL, respectively. The components are mixed at the molecular level, which complies with [38]. However, in our case, the mixed state is not stable for a longer time period. The measurements carried out ten days after the sample preparation indicate that the systems separated into three phases with the repeat distances of about 33.6, 42, and 47 Å during this time.

The phase with a repeat distance of 33.6 Å has been assigned to CHOL separated into CHOL monohydrate crystals [32]. This separation of CHOL from membranes was described also in the neat SC [39].

The S-phase with a periodicity of about 42 Å was difficult to interpret. A similar phase separation was observed in other studies [40], where, besides the phase-separated CHOL, two other phases with periodicity of about 54 and 41 Å, respectively, were described, too. The phase separation into the L- and S- phase indicates limited miscibility between the membrane components at low temperatures. Formation of separated free fatty acid- and ceramide-rich domains at temperatures below 40°C has been described in SC-lipid model mixtures by IR and ^{2}H NMR spectroscopy [6,41,42] and confirms the domain mosaic SC organization proposed by Forslind [43].

We suppose that the S-phase in our system is composed mainly of palmitic acid, a free fatty acid with a relatively short chain. It was described that while fatty acids with C14-18 chains can induce such a phase separation in a system of isolated SC lipids, the longer fatty acids (C20-26) are fully miscible with the other membrane components [44]. This phenomenon has been interpreted by the mismatch in chain lengths of fatty acids and ceramides. Interestingly, a similar effect occurs in our study although the chain length of the ceramide used is

comparable with the chain length of palmitic acid. Thus, the observed phase separation does not seem to be connected merely with the differences in the chain lengths.

It is difficult to define from the present data whether the S-phase includes only the neat palmitic acid or also other components of the mixture. Nevertheless, the content of CHOL incorporated in the S-phase is probably very limited, because only a minimum influence of the CHOL concentration on the lamellar repeat distance of the S-phase has been detected. Furthermore, a limited miscibility between free fatty acid and CHOL has been described [8].

The influence of CHOL concentration on the membrane structure has been studied. The well-mixed system originating after heating shows a high sensitivity of the lamellar repeat distance on the CHOL content. In the concentration range used, the periodicity of the lamellar phase decreases with increasing content of CHOL in the system. This dependence seems to have a linear tendency. A similar effect has been described elsewhere [45]. Moreover, our results show that in the liquid-crystalline phase (at 85 °C), CHOL contrarily increases the periodicity. This fact excludes the possibility that CHOL decreases the membrane thickness only because its molecule is smaller than that of the long-chain components.

The effect of CHOL on the hydration of the polar head groups of the membrane is improbable, too. If the change of water layer between the membranes would be responsible for the decreasing periodicity with increasing CHOL content, the real membrane thickness would not change as it has been detected by SANS. Furthermore, the water layer between the membranes was described to be extremely thin (about 1.5 Å under full hydration) in comparison to other biological membranes [16].

The most probable explanation of the CHOL effect on the membrane properties is that at 32 °C, CHOL decreases the order of the well ordered hydrocarbon chains which causes a higher fluidity in the membrane. This is accompanied by the decrease in the membrane thickness. Also the finding that the area per molecule of the membrane surface increases with the increasing CHOL concentration in the system supports our hypothesis. The

increasing area/molecule of the membrane surface indicate that the intermolecular interactions between the particular lipids (H-bonds in the head group region) weaken, which is again connected with the increase in the membrane fluidity. This is in accordance with other authors [46].

On the contrary, in the liquid-crystalline phase, CHOL increases the periodicity, which is a consequence of the increasing chain order. A similar hypothesis was proposed previously [6].

The question is why CHOL does not show this effect in the phase-separated state with well-ordered chains before heating. The S-phase is almost not affected and the periodicity of the L-phase increases slightly with increasing CHOL content. It can be connected with the fact that in this state, a considerable portion of CHOL is separated into CHOL monohydrate crystals and the CHOL amount incorporated in the other phases is limited.

As mentioned above, the SANS measurements enabled us to determine the membrane thickness and to confirm that it decreases with increasing CHOL concentration in the membrane. The minimum at q_{Rmin} related to the average vesicle radius which is normally observable in SANS curves of phospholipid vesicles [27,47], did not occur in the scattering curves in any of the samples measured. This indicates that the vesicle radii of the SC lipid ULVs are larger than the detection limit of the SANS measurements (about 600 Å). This fact implies that the SC lipid model membrane is more rigid than that of phospholipid systems, because the membrane properties do not allow to create a higher curvature. Interestingly, the hydrodynamic vesicle radius according to DLS data was also found to be about 600 Å. For comparison, dimyristoylphosphatidylcholine vesicles show a much larger hydrodynamic radius revealed by DLS as the radius measured by SANS [47,48]. The difference is due to the hydration layer on the vesicle surface. The fact that the SC lipid model vesicles do not show a difference between both radii suggests that the hydration layer on the vesicle surface is minimal.

5 Conclusions

The present study describes the phase behaviour of SC lipid model membranes in MLVs and ULVs. The influence of CHOL on the lamellar repeat distance has been studied. Immediately after the sample preparation, the membranes show one lamellar phase. During next days, the systems separate into three phases, one with a lamellar spacing of 33.6 Å consists predominantly of crystalline CHOL. The other two phases with a periodicity of 41.5 Å and 46.5 Å, respectively, are barely affected by variation of the CHOL content in the membrane. Due to heating the systems over the temperature of the main phase transition, the different phases merge into one with a periodicity of about 42.5 Å. This value increases slightly with increasing CHOL concentration. After heating, the lipids remain in one phase with a periodicity of about 45.5 Å in the membrane. The lamellar spacing of this phase decreases with increasing CHOL concentration.

SANS on ULVs seems to be a powerful method for the SC lipid research, which allows one to determine the membrane thickness parameter and the area of the membrane surface per molecule. An increase in CHOL concentration in the membrane causes a reduction of the membrane thickness and an increase in the surface area per molecule.

The present data support the hypothesis that CHOL decreases the order of the well ordered hydrocarbon chains in the state below the main phase transition and increases the order of chains in the liquid crystalline phase.

Acknowledgements

The work was supported by grant of the Federal State of Saxony-Anhalt (Project 3482A/1102L). The financial assistance from the Grant agency of the Czech Republic (GACR 202/07/P391) is gratefully acknowledged. We thank to Cosmoferm B.V. (Delft, The Netherlands) for the gift of Cer [AP]. Thanks are also extended to Dr. Christoph Wagner for his assistance with the X-ray measurements as well as to DESY and GKSS Research Centre for the travel and accommodation reimbursements.

Figures:

Fig. 1: Chemical structure of Cer[AP].

Fig. 2: X-ray diffraction patterns from the systems with 25 and 10% CHOL measured three hours after the sample preparation.

Fig. 3: X-ray diffraction patterns of the SC lipid model system with various cholesterol concentrations; 20% of lipids in Tris buffer (pH=9) at [a] 32 °C before heating, [b] 85 °C, and [c] 32 °C after heating. From bottom to top: *(i)* 10% cholesterol, *(ii)* 15% cholesterol, *(iii)* 20% cholesterol, *(iv)* 25% cholesterol, and *(v)* 30% cholesterol. The Arabic numerals label the particular reflections of the S-phase; the Roman numerals label the particular reflections of the L-phase; the asterisks label the cholesterol reflections.

Fig. 4: Lamellar repeat distance of the SC lipid model system with various cholesterol concentrations measured at 32 °C before heating (filled triangles), 85 °C (partly filled circles), and 32 °C after heating (open squares). The repeat distance was calculated using a Lorentzian function to fit the first order of diffraction.

Fig. 5: Recovery of the system with 25% CHOL (mixture IV) into the phase-separated state. From bottom to top: system measured (*i*) 20 minutes after the heating, (*ii*) 1 day after the heating, (*iii*) 10 days after the heating.

Fig. 6: The size distribution of the mixture IV (25% cholesterol); 1% (w/w) of lipids in D_2O buffer extruded through 500 Å filters.

Fig. 7: [a] Neutron scattering curves of the SC lipid model system with various cholesterol concentrations. The dashed line is a guide to the eye in order to emphasize the shift in the q_{dmin} position. From bottom to top: 10% cholesterol (filled squares), 15% cholesterol (open circles), 25% cholesterol (filled triangles), and 30% cholesterol (open triangles). [b] The corresponding Kratky-Porod plots of the SANS curves (Legend: as [a]).

Fig. 8: [a] Membrane thickness parameter of the SC lipid model system in the dependence of cholesterol concentration calculated from the scattering curves as d according to the ‘model

of separated form factors' (filled squares) and d_g according to the Guinier approximation (open circles). [b] Average area of membrane surface per molecule in the dependence of cholesterol concentration.

References

[1] M.Ponec, A. Weerheim, P. Lankhorst, P. Wertz, New acylceramide in native and reconstructed epidermis, J. Invest. Dermatol. ,120 (2003) 581-588.

[2] D. Webster, J.T. France, L.J. Shapiro, R. Weiss, X-linked ichthyosis due to steroid-sulphatase deficiency, Lancet 1, 8055 (1978) 70-72.

[3] M.L. Williams, P.M. Elias, Stratum corneum lipids in disorders of cornification, J. Clin. Invest., 68 (1981) 1404-1410.

[4] E. Zettersen, M.-Q. Man, J. Sato, M. Denda, A. Farell, R Ghadially, M.L. Williams, K.R. Feingold, P.M. Elias, Recessive X-linked ichthyosis: Role of cholesterol-sulphate accumulation in the barrier abnormality, J. Invest. Dermatol., 111 (1998) 784-790.

[5] M.L. Williams, K.R. Feingold, G. Grubauer, P.M. Elias, Ichtyosis induced by cholesterol-lowering drugs. Implications for epidermal cholesterol homeostasis, Arch. Derm. Res., 123 (1987) 1535-1538.

[6] M. Lafleur, Phase behaviour of model stratum corneum lipid mixtures: an infrared spectroscopy investigation, Can. J. Chem. ,76 (1998) 1501-1511.

[7] M. Wegener, R. Neubert, W. Rettig, S. Wartewig, Structure of stratum corneum lipids characterized by FT-Raman spectroscopy and DSC. III. Mixtures of ceramides and cholesterol, Chem. Phys. Lipids, 88 (1997) 73-82.

[8] H.-C.Chen, R. Mendelsohn, M.E. Rerek, D.J. Moore, Effect of cholesterol on miscibility and phase behavior in binary mixtures with synthetic ceramide 2 and octadecanoic acid. Infrared studies, Biochim. Biophys. Acta 1512, (2001) 345-356.

[9] E. Sparr, L. Eriksson, J.A. Bouwstra, K. Ekelund, AFM study of lipid monolayers: III. Phase behavior of ceramides, cholesterol and fatty acids, Langmuir, 17 (2001) 164-172.

[10] J. Pencer, S. Krueger, C. P. Adams, J. Katsaras, Method of separated form factors for polydisperse vesicles, J. Appl. Cryst., 39 (2006) 293-303.

[11] N. Kučerka, M.A. Kiselev, P. Balgavý, Determination of bilayer thickness and lipid surface area in unilamellar dimyristoylphosphatidylcholine vesicles from small-angle neutron scattering curves: a comparison of evaluation methods, Eur. Biophys. J., 33 (2004) 328-334.

[12] G. Ch. Charalambopoulou, T. A. Steriotis, A. Ch. Mitropoulos, K. L. Stefanopoulos, N. K. Kanellopoulos, Investigation of water sorption on porcine stratum corneum by very small angle neutron scattering, J. Invest. Dermatol., 110 (1998) 988-990.

[13] G. Ch. Charalambopoulou, P. Karamertzanis, E. S. Kikkinides, A. K. Stubos, N. K. Kanellopoulos, A. Th. Papaioannou, A Study on structural and diffusion properties of porcine stratum corneum based on very small angle neutron scattering data, Pharm. Res. 17 (2000) 1085-1091.

[14] G.Ch. Charalambopoulou, Th.A. Steriotis, Th. Hauss, K.L. Stefanopoulos, A.K. Stubos, A neutron-diffraction study of the effect of hydration on stratum corneum structure, Appl. Phys. A 74 [Suppl.] (2002) S1245-S1247.

[15] G. Ch. Charalambopoulou, Th. A. Steriotis, Th. Hauss, A. K. Stubos, N. K. Kanellopoulos Structural alterations of fully hydrated human stratum corneum, Physica B, 350 (2004) e603 – e606.

[16] M.A. Kiselev, N.Y. Ryabova, A.M. Balagurov, S. Dante, T. Hauss, J. Zbytovská, S Wartewig, R. Neubert, New insights into the structure and hydration of a stratum corneum lipid model membrane by neutron diffraction, Eur. Biophys. J., 34 (2005) 1030-1040.

[17] G. Ch. Charalambopoulou, Th. A. Steriotis, K. L. Stefanopoulos, A. Ch. Mitropoulos, N. K. Kanellopoulos, U. Keiderling, Investigation of lipid organization on stratum corneum by

water absorption in conjunction with neutron scattering, Physica B, 276-278 (2000) 530 – 531.

[18] M.A. Kiselev, P. Lesieur, A.M. Kisselev, D. Lombardo, V.L. Aksenov, Model of separated form factors for unilamellar vesicles, Appl. Phys. A, 74 (2002) S1654-S1656.

[19] W. Knoll, J. Haas, H.B. Stuhrmann, H.-H. Fuldner, H. Vogel, E. Sackmann. Small-angle neutron scattering of aqueous dispersions of lipids and lipid mixtures. A contrast variation study, J. Appl. Cryst., 14 (1981) 191-202.

[20] L.A.Feigin, D.I. Svergun, Structure analysis by small-angle X-ray and neutron scattering, Plenum Publishing Corporation, New York, 1987.

[21] R.M. Hatfield, L.W.M. Fung, Molecular properties of a stratum corneum model lipid system: large unilamellar vesicles, Biophys. J., 68 (1995) 196-207.

[22] W. Abraham, D.T. Downing, Preparation of model membranes for skin permeability studies using stratum corneum lipids, J. Invest. Dermatol., 93 (1989) 809-813.

[23] R.R.C. New, Liposomes – a practical approach. IRL Press at Oxford University Press, Oxford, New York, Tokyo, 1990.

[24] H. Farwanah, R. Neubert, S. Zellmer, K. Raith, K., Improved procedure for the separation of major stratum corneum lipids by means of automated multiple development thin-layer chromatography, Journal of Chromatography B, 780 (2002) 443-450.

[25] P. Balgavý, M. Dubničková, N. Kučerka, M.A. Kiselev, S.P. Yaradaikin, D. Uhríková, Bilayer thickness and lipid interface area in unilamellar extruded 1,2-diacylphosphatidylcholine liposomes: a small-angle neutron scattering study, Biochim. Biophys. Acta, 1512 (2001) 40-52.

[26] M.A. Kiselev, D. Lombardo, A.M. Kisselev, P. Lesieur, V.L. Aksenov, Structure factor of dimyristoylphosphatidylcholine unilamellar vesicles: small-angle X-ray scattering study. Poverhnost, 11 (2003) 20-24 (written in Russian).

[27] M.A. Kiselev, J. Zbytovská, D. Matveev, S. Wartewig, I.V. Gapienko, J. Perez, P. Lesieur., A. Hoell, R. Neubert, Influence of trehalose on the structure of unilamellar DMPC vesicles, Colloids and Surfaces A, 256 (2005) 1-7.

[28] V.M. Garamus, J.S. Pedersen, H. Kawasaki, H. Maeda, Scattering from polymer like micelles of TDAO in salt/water solutions at semidilute concentrations. Langmuir, 16 (2000) 6431-6437.

[29] K. Vávrová, J. Zbytovská, K. Palát, T. Holas, J. Klimentová, A. Hrabálek, P. Doležal, Ceramide analogue 14S24 ((S)-2-tetracosanoylamino-3-hydroxypropionic acid tetradecyl ester is effective in skin barrier repair in vitro, Eur. J. Pharm. Sci., 21(2004) 581-587.

[30] N. Bodor, Z. Gabanyi, C. Wong, A new method for the estimation of partition coefficients, J. Am. Chem. Soc., 111 (1989) 3783–3786.

[31] A. Gavezzotti, The calculation of molecular volumes and the use of volume analysis in the investigation of structured media and of solid state organic reactivity, J. Am. Chem. Soc., 105 (1983) 5220–5225.

[32] B.M. Craven, Crystal structure of cholesterol monohydrate, Nature, 260 (1976) 727-729.

[33] E. Ayranci, G. Akgul, Apparent molar volumes and viscosities of lauric, palmitic, and stearic acids in 2-butanol at (20, 30, 40, and 60) °C, J. Chem. Eng. Data, 48 (2003) 56-60.

[34] P. Góralski, M. Wasiak, Influence of van der Waals interactions on volumetric properties of cholesterol in solvents of linear structure, J. Chem. Thermodynamics, 35 (2003) 1623-1634.

[35] Y. Chevalier, Y. Zemb, The structure of micelles and microemulsions. Rep. Prog. Phys., 53 (1990) 279-371.

[36] D.T. Downing, W. Abraham, B. Wegner, K.W. Willman, J.E. Marshall, Partition of sodium dodecyl sulphate into stratum corneum lipid liposomes, Arch. Dermatol. Res., 285 (1993) 151-157.

[37] R.M. Hatfield, L.W.M. Fung, A new model system for lipid interaction in stratum corneum vesicles: effects of lipid composition, calcium, and pH, Biochemistry, 38 (1999) 784-791.

[38] M. E. Rerek, D. Van Wyck, R. Mendelsohn, D. J. Moore, FTIR spectroscopic studies of lipid dynamics in phytosphingosine ceramide models of the stratum corneum lipid matrix, Chem. Phys. Lipids, 134 (2005) 51-58.

[39] J.A. Bouwstra, G.S. Gooris, W. Bras, D.T. Downing, Lipid organization in pig stratum corneum, J. Lipid. Res., 36 (1995) 685-695.

[40] J.A. Bouwstra, J. Thewalt, G.S. Gooris, N. Kitson, A model membrane approach to the epidermal permeability barrier: an X-ray diffraction study, Biochemistry, 36 (1997) 7717-7725.

[41] D.J. Moore, M.E. Rerek, Insights into the molecular organization of lipids in the skin barrier from infrared spectroscopy studies of stratum corneum lipid models, Acta Derm. Venerol. Supp., 208 (2000) 16-22.

[42] N. Kitson, J. Thewalt, M. Lafleur, M. Bloom, A model membrane approach to the epidermal permeability barrier, Biochemistry, 33 (1994) 6707-6715.

[43] B. Forslind, A domain mosaic model of the skin barrier, Acta Derm. Venerol., 74 (1994) 1-6.

[44] J.A. Bouwstra, G.S. Gooris, K. Cheng, A. Weerheim, W. Bras, M. Ponec, Phase behaviour of isolated skin lipids, J. Lipid. Res., 37 (1996) 999-1011.

[45] J.A. Bouwstra, G.S. Gooris, F.E.R. Dubbelaar, A.M. Weerheim, A.P. Ijzerman, M. Ponec, Role of ceramide 1 in the molecular organization of the stratum corneum lipids. J. Lipid Res., 39 (1998) 186-196.

[46] H. Mizushima, J.-I. Fukasawa, T. Suzuki, Phase behaviour of artificial stratum corneum lipids containing a synthetic pseudo-ceramide: a study of the function of cholesterol, J. Lipid. Res., 37 (1996) 361-367.

[47] J. Zbytovská, M.A. Kiselev, S.S. Funari, V. Garamus, S. Wartewig, R. Neubert, Influence of phytosphingosine-type ceramides on the structure of DMPC membrane, Chem. Phys. Lipids, 138 (2005) 69-80.

[48] M.A.Kiselev, S. Wartewig, M. Janich, P. Lesieur, A.M. Kiselev, M. Ollivon, R. Neubert,. Does sucrose influence the properties of DMPC vesicles?, Chem. Phys. Lipids, 123 (2003) 31-44.

Table 1: Lipid composition of the model systems (in weight %). The concentration of cholesterol in ULVs after extrusion is given in brackets.

Lipid	I	II	III	IV	V
cholesterol	10 (8.6)	15 (14.2)	20 (-)*	25 (21.6)	30 (27)
ceramide[AP]	66	62.3	58.7	55	51.3
palmitic acid	18	17	16	15	14
cholesterol sulfate	6	5.7	5.3	5	4.7

* not measured.

Table2

Table 2: Lamellar repeat distances calculated from the X-ray diffraction patterns for the mixtures I-V. The Roman numerals in brackets describe the particular reflections.

Sample	Lamellar repeat distance [Å] (reflections [$Å^{-1}$])		
(cholesterol content)	32 °C before heating	85 °C	32 °C after heating
Mixture I (10%)	**33.6** (I: 0.187) **41.7** (I: 0.151; II: 0.306; III: 0.453) **46.7** Å (I: 0.135; II: 0.272; III: 0.405)	**41.8** (I: 0.150; III: 0.451)	**47.6** Å (I: 0.132; III: 0.397)
Mixture II (15%)	**33.6** (I: 0.187) **41.8** (I: 0.150; II: 0.309; III: 0.454) **47.0** (I: 0.134; II: 0.267; III: 0.405)	**33.6** (I: 0.187) **42.3** (I: 0.149; III: 0.446)	**33.6** (I: 0.187) **46.9** (I: 0.134; III: 0.403)
Mixture III (20%)	**33.6** (I: 0.187) **41.9** (I: 0.150; II: 0.304; III: 0.454) **47.2** (I: 0.133; II: 0.265; III: 0.404)	**33.6** (I: 0.187) **42.7** (I: 0.147; III: 0.441)	**33.6** (I: 0.187) **46.3** (I: 0.136; III: 0.408)
Mixture IV (25%)	**33.6** (I: 0.187; II: 0.370) **41.9** (I: 0.150; III: 0.455) **47.3** (I: 0.133; III: 0.396)	**33.6** (I: 0.187) **42.7** (I: 0.147; III: 0.441)	**33.6** (I: 0.187) **45.5** (I: 0.138; III: 0.413)
Mixture V (30%)	**33.6** (I: 0.187; II: 0.370) **41.9** (I: 0.150; II: 0.306; III: 0.455) **47.5** Å (I: 0.132; II: 0.263; III: 0.394)	**33.6** (I: 0.187) **42.8** (I: 0.147; III: 0.439)	**33.6** (I: 0.187) **44.9** (I: 0.140 Å; III: 0.419)

Table3

Table 3: The average excess scattering-length density ($\Delta\rho_m$) of the lipid mixtures in D_2O calculated per 1g of lipids.

Mixture	$\Delta\rho_m * 10^{10}$ [cm*g^{-1}]
I (10% CHOL)	-6.198
II (15% CHOL)	-6.189
IV (25% CHOL)	-6.170
V (30% CHOL)	-6.159

Table4

Table 4: Membrane parameters of the SC lipid model systems in dependence of cholesterol concentration calculated from the scattering curves according to the 'model of separated form factors' and the Guinier approximation.

Evaluation method	Model of separated form factors		Guinier approximation		
System	q_{dmin} [Å^{-1}]	d [Å]	R_g^2 [Å^2]	d_g [Å]	Area/molecule [Å^2]
I (10 / 8.6)*	0.170±0.009	36.9±1.9	124.7±2.5	38.7±0.8	55.2
II (15 / 14.2)*	0.172±0.009	36.4±1.8	121.3±2.4	38.2±0.8	57.3
IV (25 / 21.6)*	0.178±0.009	35.3±1.8	103.7±2.1	35.3±0.7	61.7
V (30 / 27)*	0.181±0.009	34.6±1.7	95.5±1.9	33.9±0.7	68.1

* % of cholesterol before and after extrusion.

q_{dmin}: membrane thickness minimum, d: membrane thickness parameter calculated from the q_{dmin} position, R_g: gyration radius, d_g: membrane thickness parameter calculated from the R_g-values.

Figure1

Click here to download high resolution image

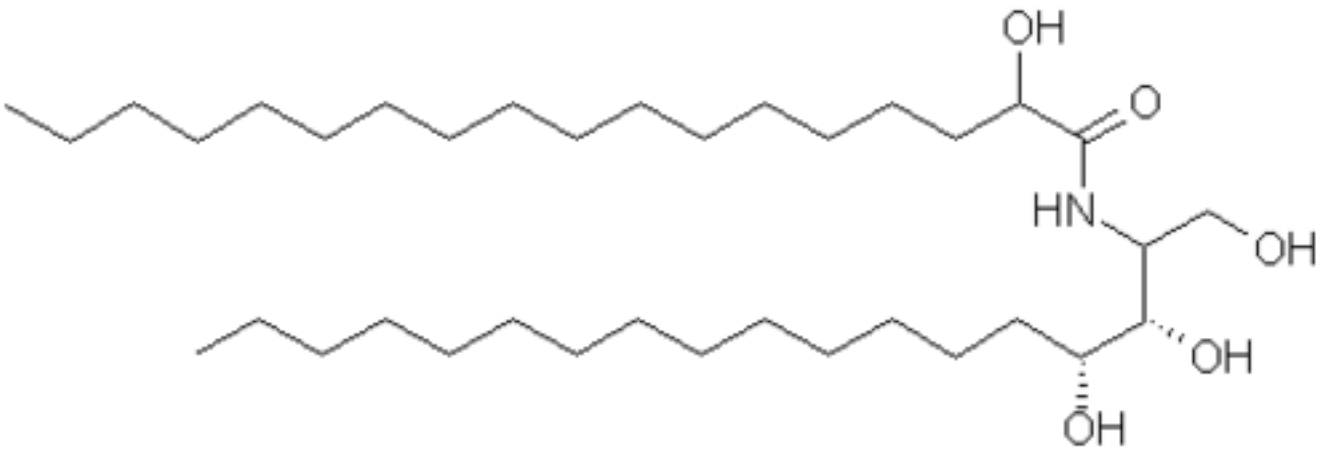

Figure2

Click here to download high resolution image

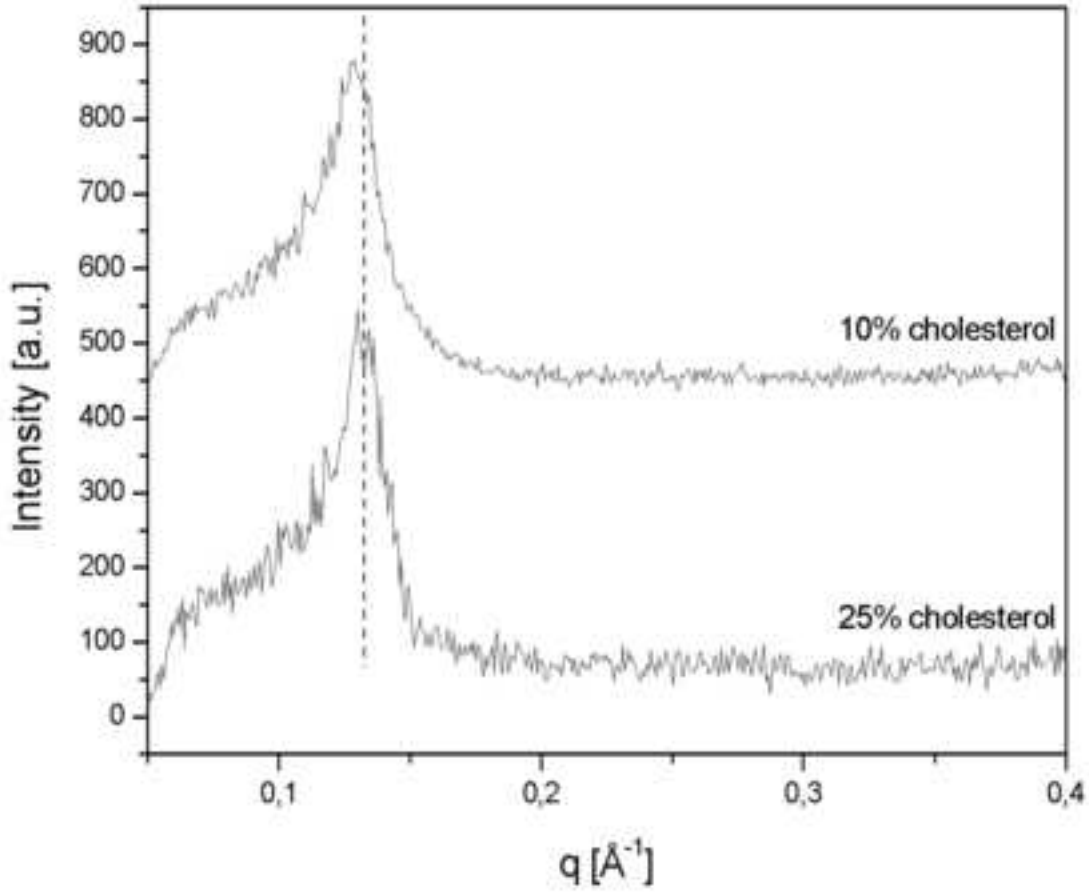

Figure3a

Click here to download high resolution image

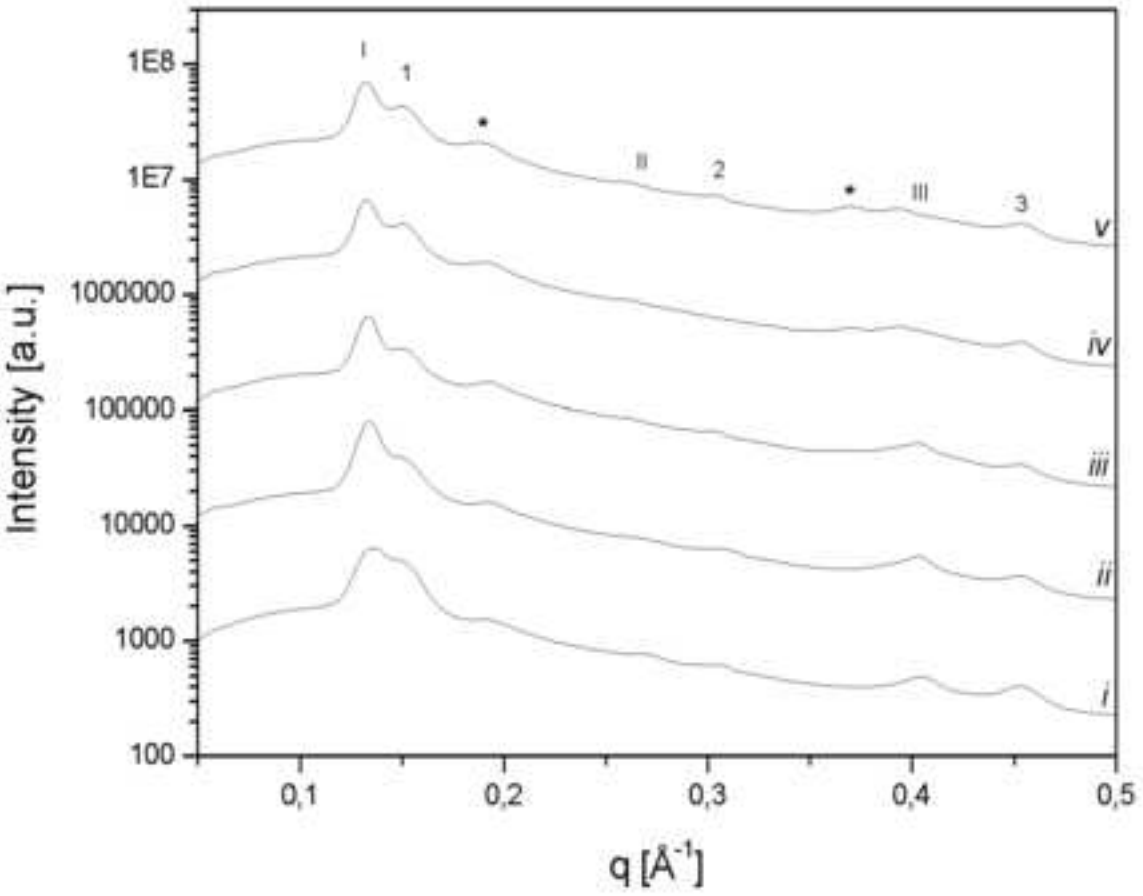

Figure3b

Click here to download high resolution image

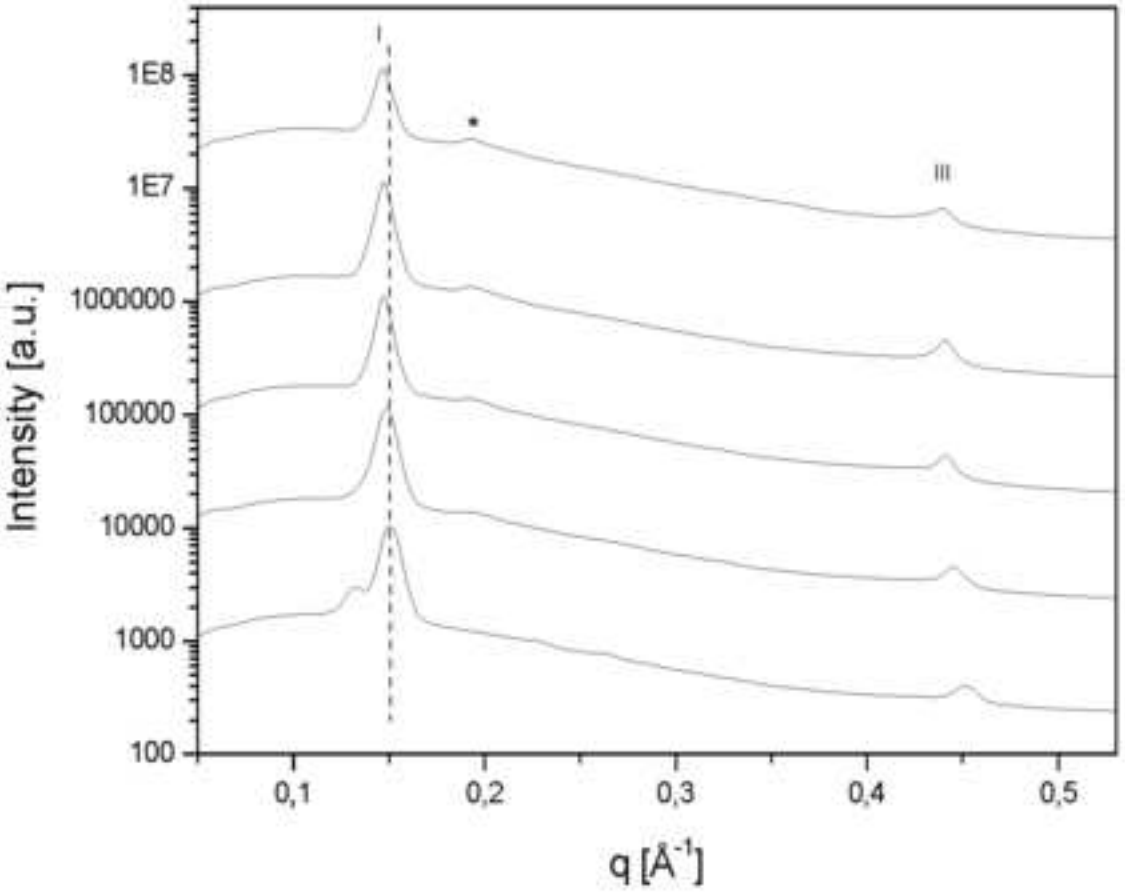

Figure3c

Click here to download high resolution image

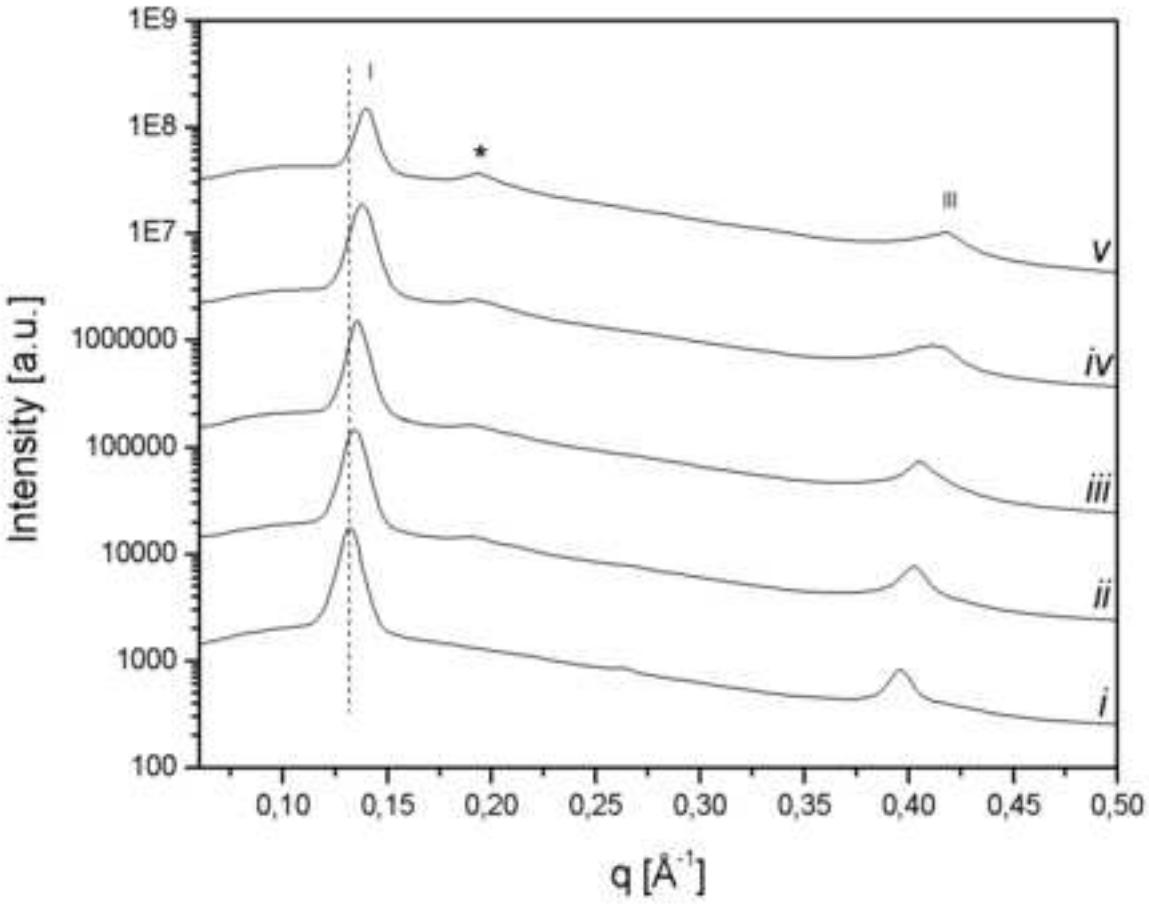

Figure4

Click here to download high resolution image

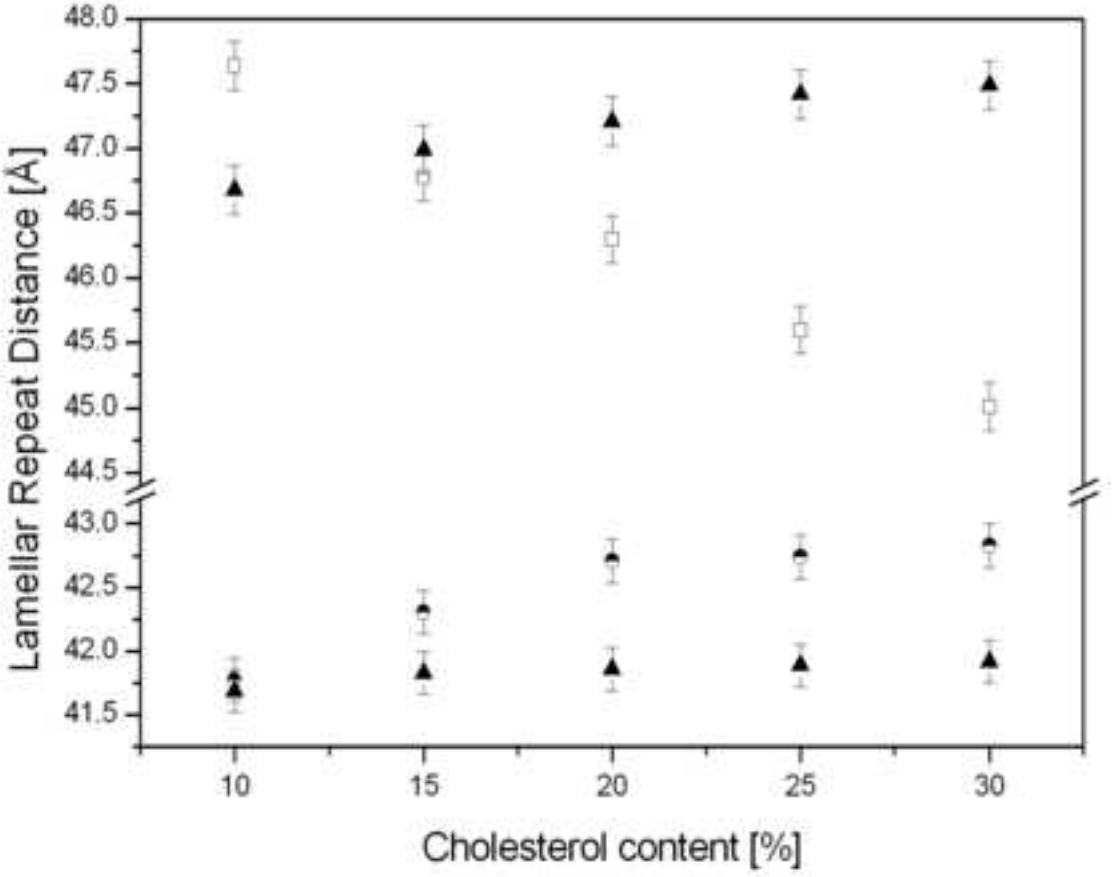

Figure5

Click here to download high resolution image

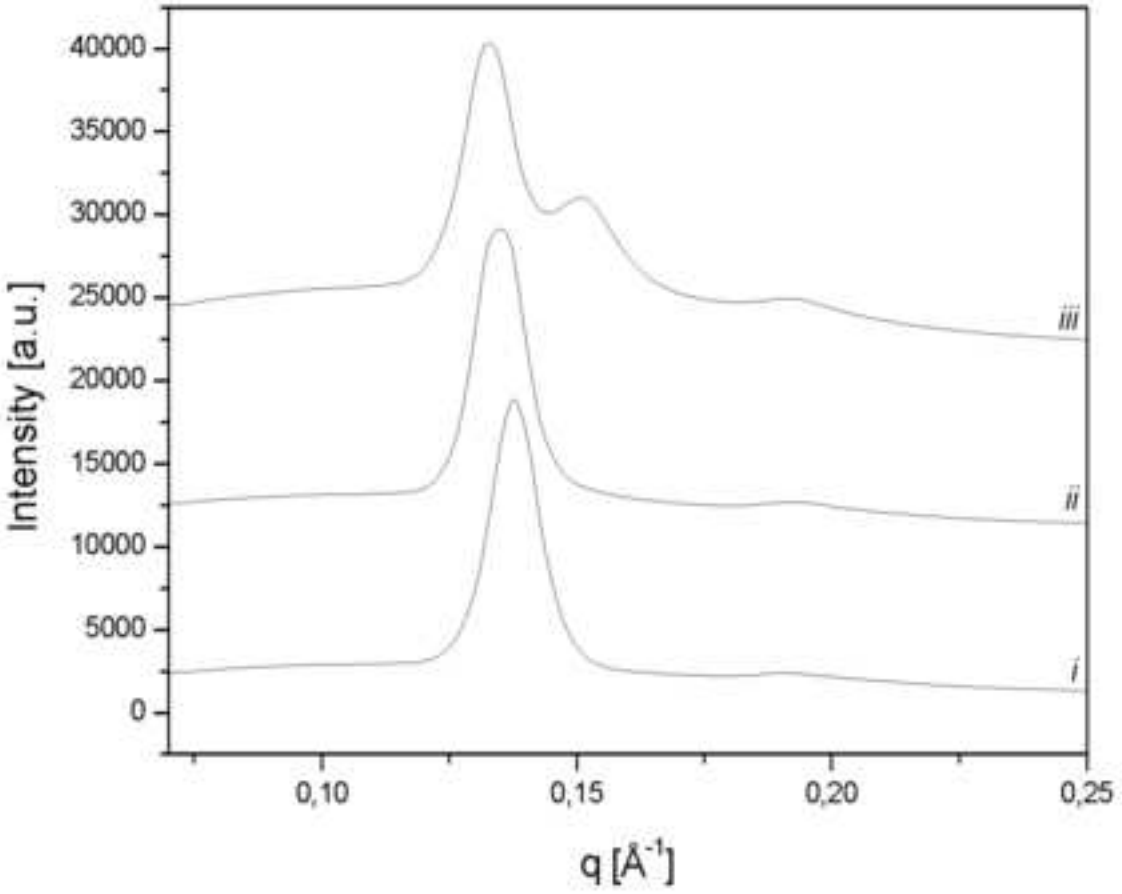

Figure6

Click here to download high resolution image

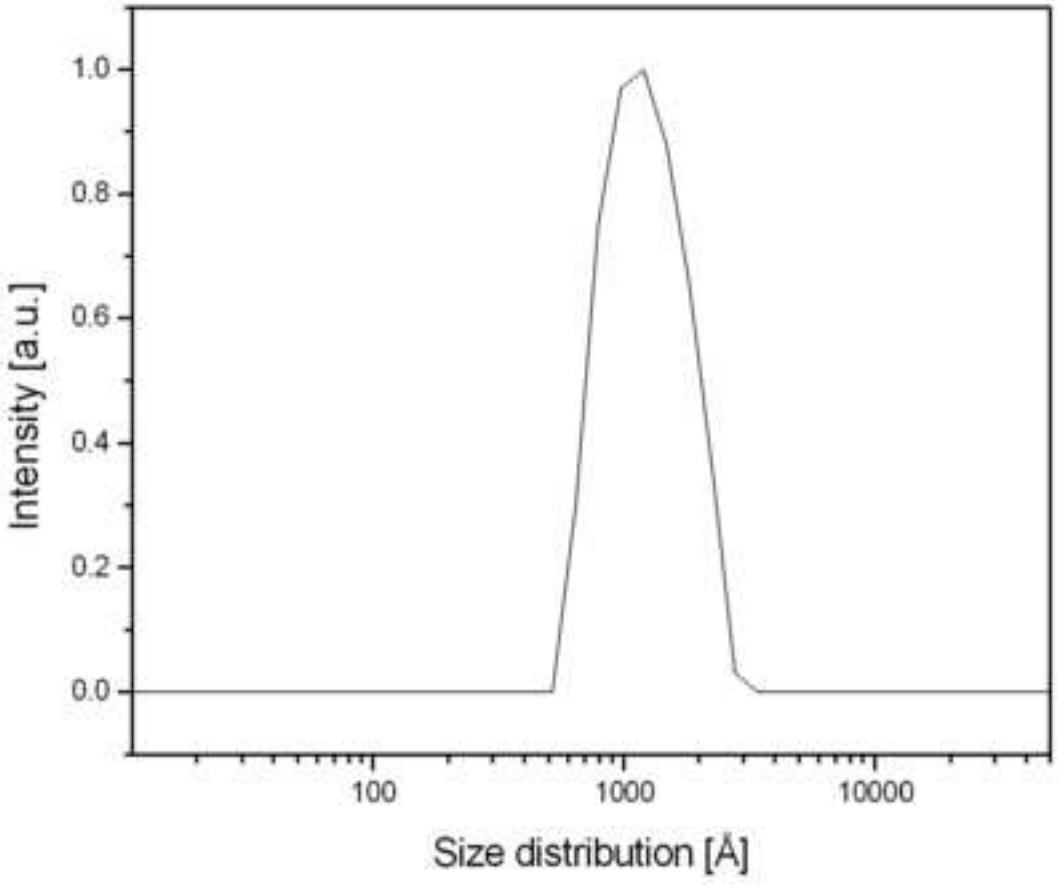

Figure7

Click here to download high resolution image

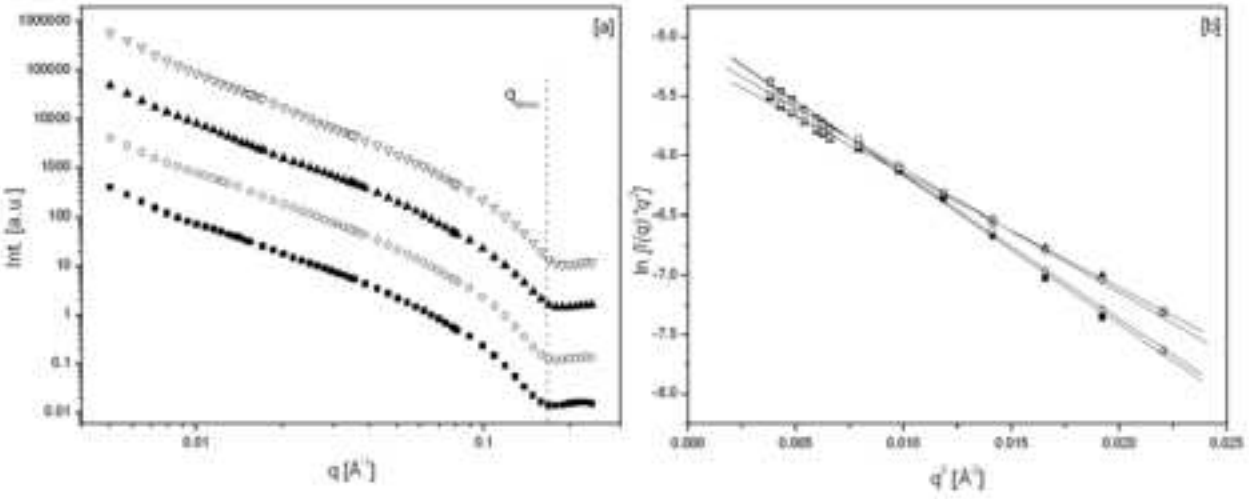

Figure8

Click here to download high resolution image